FEBS Letters 514 (2002) 90–95 FEBS 25796

RNA aptamers directed against release factor 1 from *Thermus thermophilus*

Karol Szkaradkiewicz[a], Matthias Nanninga[a], Martina Nesper-Brock[a], Michael Gerrits[b], Volker A. Erdmann[b], Mathias Sprinzl[a,*]

[a] *Laboratorium für Biochemie, Universität Bayreuth, Universitätsstraße 30, D-95440 Bayreuth, Germany*
[b] *Institut für Chemie/Biochemie, Freie Universität Berlin, Thielallee 63, D-14195 Berlin, Germany*

Received 10 November 2001; revised 29 November 2001; accepted 30 November 2001

First published online 25 January 2002

Edited by Lev Kisselev

Abstract An in vitro selection/amplification (SELEX) was used to generate RNA aptamers that specifically bind *Thermus thermophilus* release factor 1 (RF1). From 31 isolated clones, two groups of aptamers with invariable sequences 5′-ACCU-3′ and 5′-GAAAGC-3′ were isolated. Chemical and enzymatic probing of the structure indicate that in both groups the invariable sequences are located in single-stranded regions of hairpin structures. Complex formations between RF1 and aptamers of both groups were identified by electrophoretic shift assay and chemical footprinting. Deletion of the invariable sequences did not effect the secondary structure of the aptamers but abolished their binding to RF1. RNA motifs matching the invariable sequences of the aptamers are present as consensus sequences in the peptidyl transferase center of 23S rRNAs. *T. thermophilus* RF1 recognizes UAG stop codons in an *Escherichia coli* in vitro translation system. Aptamers from both groups inhibited this RF1 activity.

Key words: In vitro translation; Release factor 1; RNA aptamer; Ribosome; Peptidyl transferase

1. Introduction

Termination of protein biosynthesis takes place when a stop codon encounters the ribosomal A-site. Class I release factors (RFs; RF1 and RF2 in eubacteria, aRF1 in archaea and eRF1 in eukarya) recognize stop codons and promote the hydrolysis of the ester bond between tRNA bound in the ribosomal P-site and the nascent polypeptide chain [1]. RF1 is responsible for termination at UAA and UAG stop codons, while RF2 interacts with UAA and UGA [2]. In contrast, archaeal and eukaryotic RF1s recognize all three stop codons. Class II RFs (RF3 in eubacteria, eRF3 in eukaryotes) are GTP-binding proteins and stimulate termination by acceleration of the dissociation of RF1 and RF2 from the ribosome after cleavage of the peptidyl-tRNA [3].

Tertiary structures that mimic tRNA have been proposed for class I RFs [4]. The class I RFs are expected to mimic the shape of a tRNA. It has been suggested that a peptide anticodon exists for the recognition of the stop codons [5]. The crystal structure of human eRF1 resembles a tRNA with domain 1 of eRF1 corresponding to the anticodon arm and domain 2 of the amino acid acceptor stem of tRNA [6]. By genetic selection and biochemical studies Ito and coworkers suggested a tripeptide sequences in *Escherichia coli* RF1 and RF2 that may determine RF specificity for stop codons [7].

Structures resembling tRNAs were also identified in the crystal structures of a part of elongation factor G (EF-G) [8–9] and the ribosomal recycling factor [10–12]. All these translation factors are supposed to interact with the ribosomal A-site. However, as the ribosomal A-site changes its conformation during a translation cycle, it is conceivable that different translation factors bind to different parts of ribosomal RNA.

Class I RFs interact with the peptidyl transferase center of the large ribosomal subunit to trigger peptidyl-tRNA hydrolysis. A highly conserved GGQ motif was proposed to participate in this reaction [13,14]. The crystal structure of eRF1 confirmed this suggestion [6].

RFs compete with suppressor tRNAs for binding to the ribosomal A-site in vitro and in vivo [15–19]. Interaction of RF1 with 16S rRNA near the decoding site was identified by footprints of RF1 on helix 31 of 16S rRNA [20]. An X-ray structure of a complex of 30S subunit and mRNA with cognate tRNA bound to the A-site revealed that codon–anticodon interaction takes place in the vicinity of helix 44 and the cloacin cleavage site (position 1493) of 16S rRNA [21–22]. Cloacin cleavage inhibits formation of a complex between ribosome, UAA triplet and RF1 or RF2 [23]. It is therefore conceivable that during termination, the part of RF1 (RF2) that recognizes the stop codon is located in the vicinity of helix 44 and 1490-region of 16S rRNA. The other end of the elongated molecule bearing the conserved GGQ motif is probably located in the domain V of 23S rRNA [24]. This protein-free site formed by five stem junctions was identified as the catalytic center of the peptidyl transferase reaction [25].

Previously, selection of RNA aptamers that bind to EF-Tu provided hints for the interaction of EF-Tu with the α-sarcin/ricin region of 23S rRNA [26]. In the present work the same RNA selection/amplification approach was used to identify invariant sequences in RNA aptamers directed against *Thermus thermophilus* RF1. As the concentration of available RF1 (RF2) influences the efficiency of stop codon recognition, the effect of RF1 depletion by RNA aptamers on the recognition of a stop codon was tested in an in vitro translation system.

*Corresponding author. Fax: (49)-921-552432.
E-mail address: mathias.sprinzl@uni-bayreuth.de (M. Sprinzl).

0014-5793/02/$22.00
PII: S0014-5793(02)02308-6

2. Materials and methods

2.1. Materials

T7 polymerase was prepared as described by Zawadzki and Gross [27]. AMV reverse transcriptase was from U.S. Biochemicals Corp. (Cleveland, OH, USA). Taq polymerase was from PeqLab (Erlangen, Germany). Ni-NTA agarose was purchased from Qiagen (Hilden, Germany). Other analytical grade chemicals were obtained from Merck (Darmstadt, Germany). Radioactive nucleotides and [^{35}S]L-methionine (37 TBq/mmol) were purchased from Hartmann Analytic (Braunschweig, Germany).

2.2. Construction of N-terminally histidine-tagged RF1 from T. thermophilus

Vector pET28c (Novagen, Madison, WI, USA) was used for the construction of the plasmid pET28prfA for expression of RF1 in *E. coli*. Cell growth and cell lysis were performed as described [28]. The crude cell extract was incubated at 65°C for 20 min. After centrifugation the supernatant was dialyzed against 50 mM Tris–HCl, pH 7.5, 50 mM KCl, 50 mM NH_4Cl, 10 mM $MgCl_2$ and 10 mM 2-mercaptoethanol. Purification by Ni-NTA affinity column was performed as described for EF-Tu [29].

2.3. Selection of RNA

Selection of RNA was performed as described for EF-Tu-binding aptamers [26]. The affinity chromatography of RF1-binding aptamers on Ni-NTA resin was done in a buffer containing 50 mM Tris–HCl, pH 7.5, 50 mM NaCl and 7 mM $MgCl_2$. RNA aptamers obtained after eight selection/amplification cycles were reverse transcribed, cloned and sequenced.

The aptamers were tested for binding to RF1 by electrophoresis on 6% polyacrylamide gels in the absence of denaturing agents. The gel and running buffer contained 25 mM Tris-base, 25 mM acetic acid, and 5 mM magnesium acetate. Individual RNAs (200 pmol) were preincubated with 200 pmol RF1 in a total volume of 10 μl for 5 min on ice. After addition of 2 μl of loading buffer (30% (v/v) glycerol, 0.25% (w/v) xylene cyanol, bromphenol blue), the gels were run for 90 min at 100 V/12 cm at 4°C. Chemical probing of RNA structures and footprint analyses were done as described [26].

2.4. Preparation of suppressor $tRNA^{Ser}_{CUA}$ (su^+_I)

Plasmid ptSer with a gene of su^+_I under control of T7 promoter was used as a template for T7 transcription. Transcripts were purified by electrophoresis on a 8% polyacrylamide gel containing 7 M urea with 89 mM Tris–borate, pH 8.3, 2.5 mM EDTA. Bands of RNA were visualized by UV shadowing and eluted from gel slices by incubation with 300 mM sodium acetate pH 6.0. Purified su^+_I was precipitated with ethanol, dissolved in distilled water and stored at −20°C.

2.5. In vitro translation

In vitro translation was performed using the T7-S30 *E. coli* translation system described previously [30]. Plasmid $pHMFA_{Amb88}$ with the gene of bovine fatty acid-binding protein (FABP) carrying an internal in-frame UAG codon and a natural UGA termination codon, served as a template for coupled transcription and translation. Reaction mixtures (25 μl) contained 0.02 μg/μl $pHMFA_{Amb88}$, 0.37 GBq [^{35}S]L-methionine, 0.001 μg/μl rifampicin, 1 μM su^+_I and other components of S30 translation system, according to the manufacturer's instructions. Where indicated, 1 μM RF1 from *T. thermophilus* and various concentrations of aptamers were added. Reactions were incubated for 90 min at 37°C. Translation products were analyzed by SDS–PAGE on 15% polyacrylamide slab gel (20×20 cm) [31]. Prior to electrophoresis, peptides were precipitated on ice with 4 vol. of acetone for 15 min, centrifuged at 12 000×*g* for 15 min at 4°C, dried and dissolved in SDS–PAGE loading buffer. Electrophoresis was run at room temperature at 60 V for about 24 h. The radioactive trace of ^{35}S-labeled peptides was measured in a Canberra–Packard Instant Imager 2024 (Packard Instrument, Meriden, USA).

3. Results

3.1. In vitro selection of RF1-binding RNAs

RNA aptamers that bind to *T. thermophilus* RF1 were selected from a RNA library of approximately 10^{13} different RNA molecules with a variable sequence of 50 nucleotides. Selection was carried out with N-terminally His-tagged RF1 immobilized on a Ni-NTA agarose ensuring complete saturation of Ni^{2+}-sites. A pre-selection step was performed to eliminate RNA molecules capable of binding to the matrix itself [26]. A significant increase in RNA binding to the protein was detected after eight rounds of selection. This pool of RNAs was converted into cDNA, cloned and sequenced. Nine different sequences were identified in 31 sequenced clones. These could be divided into group I and II possessing a 5′-ACCU-3′ and a 5′-GAAAGC-3′ sequence, respectively (Fig. 1).

3.2. Structure of RNA aptamers and their interaction with RF1

Secondary structures of group I and group II aptamers were calculated using the program mfold [32]. These structures suggest that the invariable sequences of the respective groups are located in unpaired regions of hairpin structures. This is exemplified for RNA5 of group I, and RNA7 for group II in Fig. 2. The calculated secondary structures are in agreement with results obtained by limited treatment of RNAs with nuclease S1 which preferentially cleaves the RNA in single-stranded regions. Major S1 nuclease cuts are indicated by arrows in Fig. 2. These are located in unpaired areas that contain the invariant 5′-ACCU-3′ and 5′-GAAAGC-3′ sequences (Fig. 2; gray background).

Positions in RNA5 and RNA7 protected by RF1 were tested by hydroxyl radical footprinting (Fig. 2; filled squares).

Group I

RNA1	5'-CAAGCCGUCAGUCUG**ACCU**CGGAGCACACAGGACGACAA-3'	(2)
RNA2	5'-ACAAUAUAAUACCAAUCC**ACCU**UGUUGCACCGGAGUACAU-3'	(2)
RNA3	5'-ACAAUGUGAUACCAAUCC**ACCU**UGUUCUAAUACGACUCACUAUAGGGAGAGGAUACUACAC-3'	(3)
RNA4	5'-GGCAGGAUCGACCACG**ACCU**CGUAGCACACACUGGAGCCGC-3'	(1)
RNA5	5'-GUGUGUCAAGCCAGCCCUAGCUUGCU**ACCU**GGGGGCCACUGACCUAU-3'	(2)

Group II

RNA6	5'-ACUCCAAUGCGUGAUAUUGAG**GAAAGC**UGAAAGUGAUCGAAUCGCGCGAG-3'	(9)
RNA7	5'-**GAAAGC**UGAAAGUGAACGGAGUAUCACAGAGAACCCGGAAAAGUGGAG-3'	(4)
RNA8	5'-CAAAGAAAACGAGAGUAAAAGGCGC**GAAAGC**UCGUACG-3'	(7)
RNA9	5'-GCAUUGGCAAAUCCGGU**GAAAGC**ACAAACCGCCGCUCUGGCCUACGGAUA-3'	(1)

Fig. 1. Sequences of RF1-binding aptamers. Invariable sequences 5′-ACCU-3′ and 5′-GAAAGC-3′ are underlined. The numbers in parentheses indicate the sum of individual sequences among 31 sequenced clones.

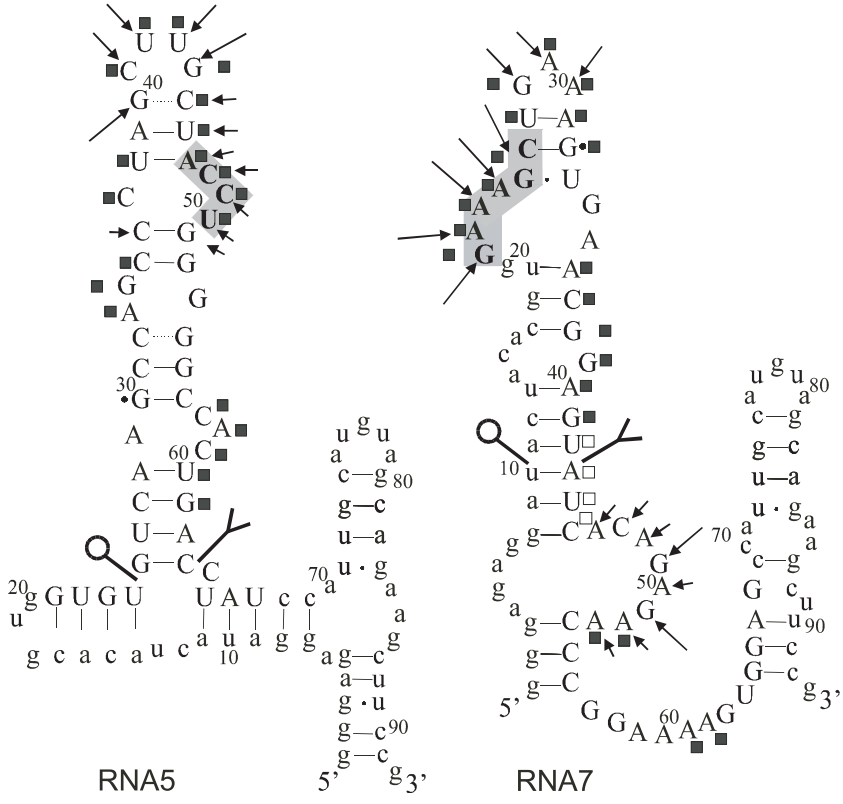

Fig. 2. Calculated secondary structures of RNA5 and RNA7. The positions of nuclease S1 cleavages are indicated by arrows. The length of arrows correlates with the intensity of the corresponding bands in PAGE. Positions protected by RF1 in hydroxyl radical footprinting are indicated by filled squares. Open squares indicate positions of increased reactivity in complex with RF1. The 3′ and 5′boundaries are labeled by (Y) and (–o), respectively.

Strong protection was observed in the unpaired regions containing the invariable sequences. Several adjacent nucleotides were also protected. This indicates that RF1 interacts with aptamers along one side of the hairpin helix that is interrupted by a single-stranded region containing the respective invariant sequence.

The minimal length of the aptamers sufficient to confer binding to RF1 was determined by affinity chromatography of 5′-end- and 3′-end-labeled aptamers that were randomly hydrolyzed. 5′-end- and 3′-end-labeling provided the 3′ and the 5′ boundaries, respectively. The boundaries for RNA5 and RNA7 shown in Fig. 2 confirm the results of hydroxyl radical footprinting. It is therefore likely that the minimal structures of RNA aptamers that confer binding to RF1 consist of a hairpin with the unpaired RF1-interacting sequence. Short RNAs that correspond to these minimal structures of RNA5 and RNA7, respectively, were chemically synthesized. These RNAs were still able to bind RF1 (data not shown).

Complex between RF1 and RNA aptamers were visualized by electrophoretic band shift assay. RF1–RNA complexes exhibit an intermediate mobility between fast-moving RNA and slow-moving protein (Fig. 3). As estimated from these band shift experiments, the dissociation constant of RF1–RNA5 and RF1–RNA7 complexes are below 2×10^{-5} M. UV-melting and chemical probing show that deletion of the 5′-ACCU-3′ consensus motif from RNA5 (ΔRNA5) does not destroy the hairpin structure, but completely abolishes RF1 binding (Fig. 3). Similar results were obtained for RNA7 after deletion of the 5′-GAAAG-3′ consensus sequence (data not shown).

3.3. *T. thermophilus RF1 is active in an E. coli in vitro translation*

As suppressor tRNA and class I RFs compete for binding to mRNA non-sense codons exposed in the ribosomal A-site, efficiency of read-through depends on the availability of RFs and suppressor tRNA. Therefore, the activity of RFs can be measured via determination of the read-through efficiency of the particular non-sense codon [18]. We examined the ability of selected RNA aptamers to modulate RF1 activity in an assay based on the abolishment of read-through of mRNA UAG codon by *T. thermophilus* RF1 in a cell-free *E. coli* 30S translation system. A gene of FABP carrying an in-frame UAG codon and a natural UGA termination codon (Fig. 4) served as a template for coupled in vitro transcription and translation. In this assay premature termination on UAG codon leads to synthesis of a termination product (9.6 kDa) (Fig. 4, lane 1), whereas read-through in the presence of Ser-su$_I^+$ results in synthesis of a suppression product, corresponding to full-length FABP (14.7 kDa). Without addition of RF1, termination on the internal UAG codon is weak (Fig. 4, lane 1). Recognition of the internal UAG codon leads to reduction of read-through mediated by suppressor Ser-su$_I^+$ and increase in synthesis of the termination product (Fig. 4, lane 3). Quantitative analysis of bands of ^{35}S-labeled peptides revealed a nearly four-fold decrease in the ratio of suppression to termination products after addition of 1 μM *T. thermophilus* RF1 to the *E. coli* S30 in vitro translation system containing 1 μM su$_I^+$. The yield of suppression product was reduced by 44% (Fig. 4, lanes 2 and 3).

Addition of RF1 to the suppressible *E. coli* in vitro translation system caused not only a reduction of the read-through and an increase of the synthesis of termination product, but also a drop of the translation yield. Total radioactivity incorporated into peptides in the presence of 1 μM RF1 was reduced by 22–26% as compared to the control experiment without RF1 (Fig. 4, lanes 2 and 3). This effect can be explained by the competition between RF1 and aminoacylated elongator tRNAs for binding to the ribosomal A-site during peptide elongation [33].

3.4. Inhibition of termination by RF1-binding aptamers

RNA5 (group I) and RNA7 (group II) aptamers were employed in the experiments shown in Figs. 5 and 6, respectively. Competition between RF1 and Ser-su_I^+ for the UAG codon defines the ratio of synthesized suppression and termination products. In both cases, the suppression/termination products ratio is significantly increased with increasing aptamer concentration. The observed increase in read-through efficiency indicates that RF1 aptamers decrease the activity of RF1 to promote termination at UAG codons. At high concentrations, RF1 aptamers also cause a reduction of the overall yield of protein synthesis. We assume that this effect is the result of ribosome stalling in absence of sufficient amount of active RF1. Although not directly proven, we expect that RF1 aptamers directed against *T. thermophilus* RF1 also bind to the *E. coli* homologue. This would decrease the recycling of ribosomes and consequently decrease the overall yield of the synthesized polypeptide.

4. Discussion

It was suggested that RF1 and RF2 mimic aminoacyl-tRNA bound to ribosomal A-site [4–5]. Both RFs interact with mRNA in the decoding site of the 30S subunit and at the same time with the peptidyl transferase center of 23S rRNA. Therefore, it can be expected that on the ribosome RF1 is involved in interactions with both rRNA and mRNA at the same time. In case that these interactions are sufficiently specific, it is conceivable that aptamers binding to RF1 with high affinity can be isolated. In turn, these aptamers are expected to correspond to either rRNA motifs present in the peptidyl transferase center or to the stop codons of mRNA. The results of the present investigation confirm this assumption. From 31 isolated clones, 13 clones of group II aptamers (RNA6 and RNA7) and five clones of group I aptamers (RNA2 and RNA3) share similar secondary structures with invariable sequences located in single-stranded regions. This indicates that RF1 possesses a surface-located structural motif that specifically recognizes certain RNA sequences. Although we did not determine the apparent dissociation constants of RF1 aptamer complexes, electrophoretic mobility shift assays (Fig. 3) suggest dissociation constants in a submicromolar range.

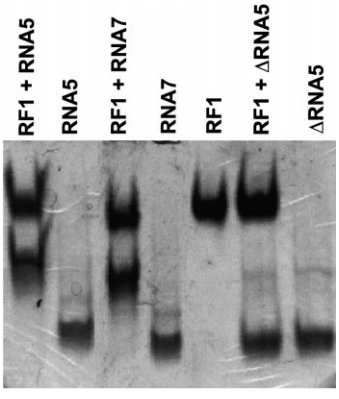

Fig. 3. Analysis of complexes formed by aptamers and RF1 by electrophoretic shift assay. ΔRNA5 is the aptamer RNA5 with deleted 5′-ACCU-3′ sequence, ΔRNA7 is the aptamer RNA7 with deleted 5′-GAAAGC-3′ sequence. For staining of protein and RNA Coomassie brilliant blue and Toluidine blue, respectively, were used.

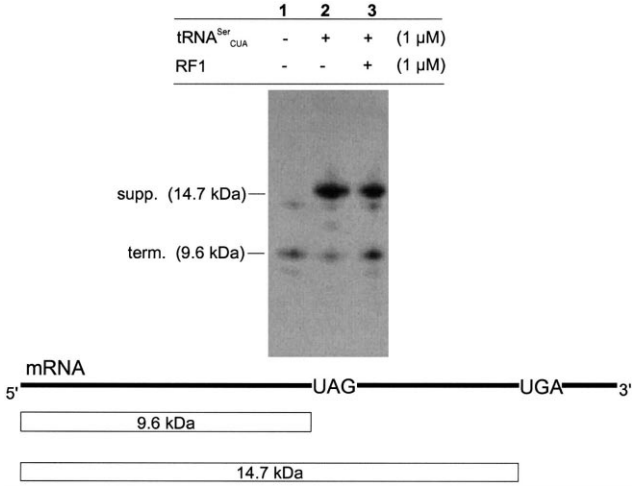

Fig. 4. In vitro RF1 for activity of RF1 based on the abolishment of read-through of an internal in-frame UAG codon. Premature termination at the UAG codon leads to synthesis of 9.6 kDa polypeptide. Suppression of this codon by Ser-su_I^+ gives rise to complete 14.7 kDa FABPs (for details see Section 2). In the upper part of the figure the SDS–PAGE products of in vitro translation in *E. coli* S30 system are shown. Bands in the autoradiography correspond to ^{35}S-labeled polypeptides. Supp. – suppression product; term. – termination product.

The functional significance of the invariable sequences in RF1 aptamers is difficult to interpret without the knowledge of the tertiary structure of RF1–ribosome complexes. However, it is remarkable that both 5′-ACCU-3′ and 5′-GAAAGC-3′ sequences occur in domain V of 23S rRNA that forms a major part of the peptidyl transferase center [22]. This implies that an interaction between RF1 and 5′-ACCU-3′ and 5′-GAAAGC-3′ within the peptidyl transferase may be involved in the hydrolysis of peptidyl-tRNA during termination. The sequence motif GGQ that is conserved in eukaryotic and prokaryotic class I RFs [6] may be located in the vicinity of the these sequences. Crosslinking performed with RNA aptamers that represent a minimal model for the peptidyl transferase may now be utilized to clarify this question.

The presence of RF1 from *T. thermophilus* in an *E. coli* in vitro translation system caused reduction of the overall yield of polypeptide synthesis and increased the formation of a correctly terminated product in relation to a suppression product. As expected, this is due to depletion of RF1 that leads to an increase in efficiency of read-through of UAG non-sense codons by su_I^+. This effect is concentration-dependent and probably reflects competition between RF1 aptamers and peptidyl transferase center for binding to RF1. Most

probably, the mechanism of RF1 inhibition by RF1 aptamers consists in mimicking the interaction site of 23S rRNA by RF1 aptamers. Formation of a RF1 aptamer complex then abolishes binding of the factor to the ribosome. This mechanism is substantiated by results of the present work and previous reports [33], which suggest that RF1 may even compete with cognate aminoacyl-tRNA for binding to the ribosomal A-site carrying sense codons during elongation steps of protein biosynthesis. This suggests further, that in addition to the interaction with UAG or UAA codons in the decoding site, some other ribosomal structures may be involved in the interaction of RF1 with the A-site.

Specific inhibition of RF1 by RF1 aptamers leads to increased efficiency of read-through of mRNA amber codons during in vitro translation. This effect may be of particular interest in all cases where increased efficiency of suppression is desirable, e.g. to facilitate incorporation of unnatural amino acids into protein via suppression of non-sense codons [33].

Recently, aptamers directed against eRF1 were isolated and tested as inhibitors of termination [34]. Although these aptamers had different structures than those presented in this work, their activity in the termination assay was similar. They inhibited termination by depletion of eRF1 from the system.

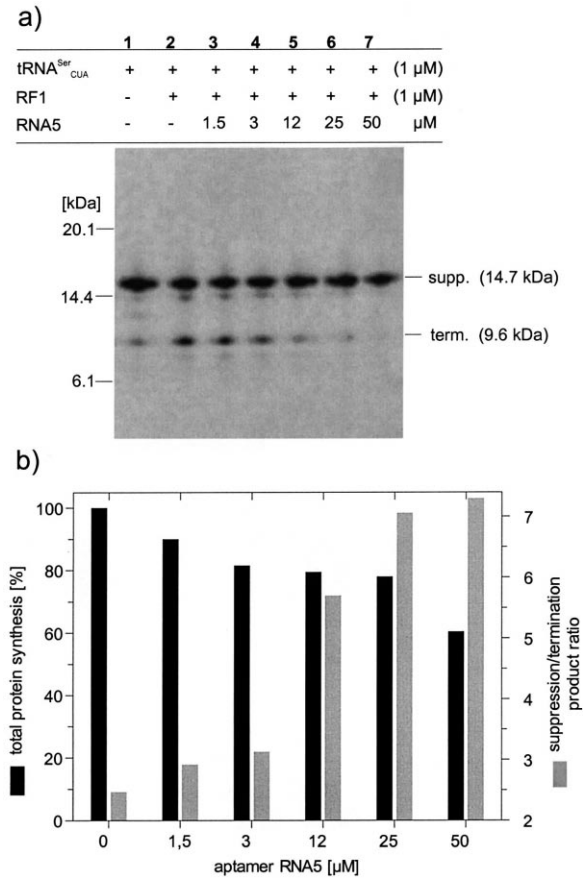

Fig. 5. Influence of aptamer RNA5 on the RF1 activity in a suppressible 30S in vitro translation system. a: SDS–PAGE of the in vitro translation products; supp. – suppression product; term. – termination product. b: Yield of translation of ^{35}S-labeled proteins (black columns) and the suppression/termination products ratio (gray columns) as a function of aptamer concentration.

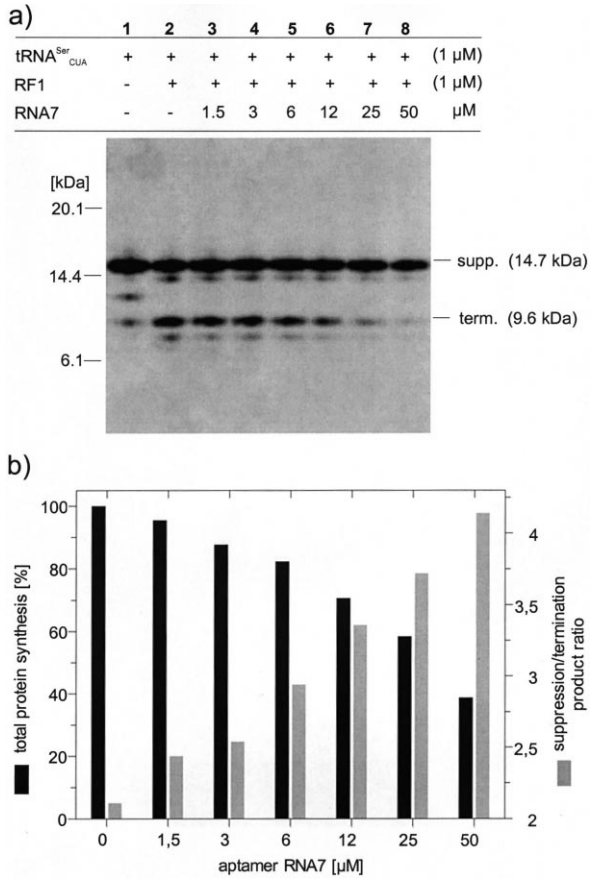

Fig. 6. Influence of aptamer RNA7 on the RF1 activity in a suppressible 30S in vitro translation system. a: SDS–PAGE of the in vitro translation products; supp. – suppression product; term. – termination product. b: Yield of translation of ^{35}S-labeled proteins (black columns) and the suppression/termination products ratio (gray columns) as a function of aptamer concentration.

Acknowledgements: This work was supported by the Deutsche Forschungsgemeinschaft Sp243/5-2 and 5-3, the European Community EC-Project BIO4-98-0189, the Bundesministerium für Bildung, Wissenschaft, Forschung und Technologie (BMFT) and the Fonds der Chemischen Industrie e.V.

References

[1] Craigen, W.J. and Caskey, T.C. (1987) Biochimie 69, 1031–1041.
[2] Scolnick, E., Tompkins, R., Caskey, T. and Nirenberg, M. (1968) Proc. Natl. Acad Sci. USA 61, 768–774.
[3] Freistroffer, D.V., Pavlov, M.Y., MacDougall, J., Buckingham, R.H. and Ehrenberg, M. (1997) EMBO J. 16, 4126–4133.
[4] Ito, K., Ebihara, K., Uno, M. and Nakamura, Y. (1996) Proc. Natl. Acad. Sci. USA 93, 5443–5448.
[5] Nakamura, Y., Ito, K. and Isaksson, L.A. (1996) Cell 87, 147–150.
[6] Seit-Nebi, A., Frolova, L., Justesen, J. and Kisselev, L.L. (2001) Nucleic Acids Res. 29, 3982–3987.
[7] Frolova, L.Y., Tsivkovskii, R.Y., Sivolobova, G.F., Oparina, N.Y., Serpinsky, O.I., Blinov, V.M., Tatkov, S.I. and Kisselev, L.L. (1999) RNA 5, 1014–1020.
[8] Song, H., Mugnier, P., Das, A.K., Webb, H.M., Evans, D.R., Tuite, M.F., Hemmings, B.A. and Barford, D. (2000) Cell 100, 311–321.
[9] Ito, K., Uno, M. and Nakamura, Y. (2000) Nature 403, 680–684.
[10] Aevarsson, A., Brazhnikov, E., Garber, M., Zheltonosova, J., Chirgadze, Y., Al-Karadaghi, S., Svensson, L.A. and Liljas, A. (1994) EMBO J. 13, 3669–3677.

[11] Nissen, P., Kjeldgaard, M., Thirup, S., Polekhina, G., Reshetnikova, L., Clark, B.F. and Nyborg, J. (1995) Science 270, 1464–1472.
[12] Selmer, M., Al-Karadaghi, S., Hirokawa, G., Kaji, A. and Liljas, A. (1999) Science 286, 2349–2352.
[13] Kim, K.K., Min, K. and Suh, S.W. (2000) EMBO J. 19, 2362–2370.
[14] Toyoda, T., Tin, O.F., Ito, K., Fujiwara, T., Kumasaka, T., Yamamoto, M., Garber, M.B. and Nakamura, Y. (2000) RNA 6, 1432–1444.
[15] Curran, J.F. and Yarus, M. (1988) J. Mol. Biol. 203, 75–83.
[16] Eggertsson, G. and Söll, D. (1988) Microbiol. Rev. 52, 354–374.
[17] Weiss, R.B., Dunn, D., Dahlberg, A.E., Atkins, J.F. and Gesteland, R.F. (1988) EMBO J. 7, 1503–1507.
[18] Drugeon, G., Jean-Jean, O., Frolova, L., Le Goff, X., Philippe, M., Kisselev, L. and Haenni, A.L. (1997) Nucleic Acids Res. 25, 2254–2258.
[19] Le Goff, X., Philippe, M. and Jean-Jean, O. (1997) Mol. Cell Biol. 17, 3164–3172.
[20] Wilson, K.S., Ito, K., Noller, H.F. and Nakamura, Y. (2000) Nat. Struct. Biol. 7, 866–870.
[21] Carter, A.P., Clemons, W.M., Brodersen, D.E., Morgan-Warren, R.J., Wimberly, B.T. and Ramakrishnan, V. (2000) Nature 407, 340–348.
[22] Ogle, J.M., Brodersen, D.E., Clemons Jr., W.M., Tarry, M.J., Carter, A.P. and Ramakrishnan, V. (2001) Science 292, 868–869.
[23] Caskey, C.T., Bosch, L. and Konecki, D.S. (1977) J. Biol. Chem. 252, 4435–4437.
[24] Ban, N., Nissen, P., Hansen, J., Moore, P.B. and Steitz, T.A. (2000) Science 289, 905–920.
[25] Nissen, P., Hansen, J., Ban, N., Moore, P.B. and Steitz, T.A. (2000) Science 289, 920–930.
[26] Hornung, V., Hofmann, H.P. and Sprinzl, M. (1998) Biochemistry 37, 7260–7267.
[27] Zawadzki, V. and Gross, H.J. (1991) Nucleic Acids Res. 19, 1948.
[28] Blank, J., Grillenbeck, N.W., Kreutzer, R. and Sprinzl, M. (1995) Protein Expr. Purif. 6, 637–645.
[29] Ribeiro, S., Nock, S. and Sprinzl, M. (1995) Anal. Biochem. 228, 330–335.
[30] Lamla, T. and Erdmann, V.A. (2001) FEBS Lett. 502, 35–40.
[31] Schägger, H. and von Jagow, G. (1987) Anal. Biochem. 166, 368–379.
[32] Zuker, M. (1989) Science 244, 48–52.
[33] Short III, G.F., Golovine, S.Y. and Hecht, S.M. (1999) Biochemistry 38, 8808–8819.
[34] Carnes, J., Frolova, L., Zinnen, S., Drugeon, G., Phillippe, M., Justesen, J., Haenni, A.L., Leinwand, L., Kisselev, L.L. and Yarus, M. (2000) RNA 6, 1468–1479.